Technical Report # MBS00-3-UIC
Department of Mechanical Engineering
University of Illinois at Chicago
June 2000

DEVELOPMENT OF A SHEAR DEFORMABLE ELEMENT USING THE ABSOLUTE NODAL COORDINATE FORMULATION

Mohamed A. Omar
Ahmed A. Shabana
Department of Mechanical Engineering
University of Illinois at Chicago
842 West Taylor Street
Chicago, IL, 60607-7022

This research was supported by the U.S. Army Research Office, Research Triangle Park, NC.

REPORT DOCUMENTATION PAGE	Form Approved OMB NO. 0704-0188

1. AGENCY USE ONLY (Leave Blank)	2. REPORT DATE November 2000	3. REPORT TYPE AND DATES COVERED Technical Report

4. TITLE AND SUBTITLE Development of a Shear Deformable Element Using the Absolute Nodal Coordinate Formulation	5. FUNDING NUMBERS DAAG55-97-1-0303
6. AUTHOR(S) Ahmed A. Shabana	
7. PERFORMING ORGANIZATION NAME(S) AND ADDRESS(ES) University of Illinois-Chicago Chicago, IL 60607-7022	8. PERFORMING ORGANIZATION REPORT NUMBER
9. SPONSORING / MONITORING AGENCY NAME(S) AND ADDRESS(ES) U. S. Army Research Office P.O. Box 12211 Research Triangle Park, NC 27709-2211	10. SPONSORING / MONITORING AGENCY REPORT NUMBER ARO 35711.27-EG

11. SUPPLEMENTARY NOTES

The views, opinions and/or findings contained in this report are those of the author(s) and should not be construed as an official Department of the Army position, policy or decision, unless so designated by other documentation.

12 a. DISTRIBUTION / AVAILABILITY STATEMENT	12 b. DISTRIBUTION CODE
Approved for public release; distribution unlimited.	

13. ABSTRACT (Maximum 200 words)

A two-dimensional shear-deformable beam element is developed in this investigation for the analysis of the large rotation and large deformation. Using the absolute nodal coordinate formulation and a continuum mechanics approach, the assumption of Euler-Bernoulli and Timoshenko beam theories are relaxed. The effect of the shear deformation is accounted for without the need for introducing Timoshenko's shear coefficient. By using the absolute coordinates, the nonlinear strain-displacement relationships are used to define a relatively simple expression for the elastic forces, while the mass matrix of the

14. SUBJECT TERMS	15. NUMBER OF PAGES
	16. PRICE CODE

17. SECURITY CLASSIFICATION OR REPORT	18. SECURITY CLASSIFICATION ON THIS PAGE	19. SECURITY CLASSIFICATION OF ABSTRACT	20. LIMITATION OF ABSTRACT
UNCLASSIFIED	UNCLASSIFIED	UNCLASSIFIED	UL

NSN 7540-01-280-5500

Standard Form 298 (Rev.2-89)
Prescribed by ANSI Std. 239-18
298-102

beam remains constant. As a consequence, the centrifugal and Coriolis forces are identically equal to zero. Surprisingly, the more general model developed in this investigation leads to a significant saving in computer time as compared to non-shear deformable models presented in previous investigations.

ABSTRACT

A two-dimensional shear-deformable beam element is developed in this investigation for the analysis of the large rotation and large deformation. Using the absolute nodal coordinate formulation and a continuum mechanics approach, the assumption of Euler-Bernoulli and Timoshenko beam theories are relaxed. The effect of the shear deformation is accounted for without the need for introducing Timoshenko's shear coefficient. By using the absolute coordinates, the nonlinear strain-displacement relationships are used to define a relatively simple expression for the elastic forces, while the mass matrix of the beam remains constant. As a consequence, the centrifugal and Coriolis forces are identically equal to zero. Surprisingly, the more general model developed in this investigation leads to a significant saving in computer time as compared to non-shear deformable models presented in previous investigations.

1. INTRODUCTION

In Euler-Bernoulli beam theory it is assumed that the cross-section remains rigid and perpendicular to the neutral axis of the beam [1, 13]. In this theory, the effect of the shear deformation is neglected. In Timoshenko beam theory on the other hand, the cross-section does not remain perpendicular to the beam neutral axis. Nonetheless, the cross-section remains rigid. A shear coefficient is introduced in order to account for the shear deformation [12]. In this investigation, a two-dimensional shear-deformable beam element based on the non-incremental absolute nodal coordinate formulation [10] is developed. In this approach, only absolute coordinates and global slopes are used to define the element nodal coordinates without the need for using infinitesimal or finite rotations. With the definition of the nodal coordinates in the global coordinate system, no transformation is required to determine the element inertia or elastic forces. Using this coordinate representation with the appropriate element shape function, exact modeling of the rigid body dynamics can be achieved. Using the non-incremental absolute nodal coordinate formulation, the resulting mass matrix of the finite element is a constant matrix and the centrifugal and Coriolis forces are identically equal to zero. Another advantage of using the absolute nodal coordinate formulation is its simplicity in formulating the generalized forces and imposing some joint constraints.

A problem encountered in the implementation of the non-incremental absolute nodal coordinate formulation is the formulation of the elastic forces. Shabana, et al [6, 8, 9, 10, 11] proposed two methods for formulating the elastic forces of the two-dimensional beam element. In the first method, a local element coordinate system is introduced for the convenience of describing the element deformation. This approach leads to a complex expression for the elastic forces even when a linear elastic model is used. In the second method [3] a continuum mechanics approach is used to obtain the elastic forces without introducing the local element coordinate system. In this continuum mechanics approach, nonlinear strain-displacement relationships must be used in order to obtain zero strain under an arbitrary rigid body motion. Nonetheless, the previous models developed using the continuum mechanics approach are based on Euler-Bernoulli beam theory which dose not account for the shear deformation. It is the objective of this

investigation to develop a model for the elastic forces for two-dimensional beam elements that accounts for shear deformation by using a general continuum mechanics approach without introducing a local element coordinate system. This new model relaxes the assumptions of Euler-Bernoulli and Timoshenko beam theories and does not require the use of a shear coefficient.

This paper is organized as follows. In section 2, the displacement field and the kinematic equations of the new two-dimensional shear-deformable beam element are presented. The constant mass matrix of the beam element that accounts for the rotary inertia is defined in section 3. In section 4, the formulation of the elastic forces using the general continuum mechanics approach is discussed. The formulations of the generalized external forces and moments associated with the element nodal coordinates using the virtual work are presented in section 5. In section 6, the equations of motion are presented and the use of the proposed model in the analysis of the large deformation of simple and multibody mechanical systems is demonstrated. Section 7 presents a summery and the conclusions drawn from the study presented in this paper.

2. KINEMATICS OF THE SHEAR-DEFORMABLE BEAM

For the two-dimensional shear-deformable beam element, the displacement field is defined in the global coordinate system as

$$\mathbf{r} = \begin{bmatrix} a_0 + a_1 x + a_2 y + a_3 xy + a_4 x^2 + a_5 x^3 \\ b_0 + b_1 x + b_2 y + b_3 xy + b_4 x^2 + b_5 x^3 \end{bmatrix} \tag{1}$$

where $\mathbf{r}$, as shown in Fig. 1, is the global position vector of an arbitrary point on the beam element cross-section, a_i and b_i are the polynomial coefficients, and x and y are the spatial coordinates defined in a beam coordinate system. The spatial coordinate x is chosen to be along the beam axis $(0 \le x \le l)$, where l is the element length. Note that, the assumed displacement field depends on y in order to account for the shear deformation.

In the simplified Euler-Bernoulli beam theory, the effect of the shear deformation is neglected [1]. The basic assumption in the simplified Euler-Bernoulli beam theory is that the cross-section of the beam remains normal to the beam neutral axis as shown in Fig. 2a. The beam cross-section at any point along the beam neutral axis can be defined by the Frenet frame. The Frenet frame has one of its axis tangent to the beam neutral axis and the other axis perpendicular to the beam neutral axis [7]. The tangent vector $\underline{\mathbf{t}}$ can be defined by $\partial \mathbf{r} / \partial x$. In a shear-deformable beam model, the cross-section of the beam does not remain normal to the neutral axis, as shown in Fig. 2b. As a result, the tangent to the neutral axis cannot be used to define the cross-section. In order to demonstrate that the shape function of Eq. 1 accounts for the shear effect, consider an arbitrary vector $\Delta\mathbf{r}$, which is defined in the beam cross-section as shown in Fig. 3. Using the displacement field defined by Eq. 1, it can be shown that

$$\Delta\mathbf{r} = \mathbf{r} - \mathbf{r}_{y=0} = y\frac{\partial \mathbf{r}}{\partial y} \tag{2}$$

where $\mathbf{r}$ is the global position vector of an arbitrary point P in the cross-section with coordinates (x,y), and $\mathbf{r}_{y=0}$ is the position vector of the corresponding point P_o on the beam centerline with coordinates $(x,0)$. The preceding equations show that any arbitrary vector drawn on the beam cross-section can be defined by the vector $\partial \mathbf{r} / \partial y$, and as a consequence the vector $\partial \mathbf{r} / \partial \mathrm{y}$ defines the cross-section of the beam. In the absolute nodal coordinate formulation, the global position vector of an arbitrary point on the beam can be written as

$$\mathbf{r} = \begin{bmatrix} r_1 \\ r_2 \end{bmatrix} = \mathbf{S}\mathbf{e} \tag{3}$$

where $\mathbf{S}$ is the global element shape function, and $\mathbf{e}$ is the vector of nodal coordinates. The vector of the element nodal coordinates $\mathbf{e}$ is given by

$$\mathbf{e} = \begin{bmatrix} e_1 & e_2 & e_3 & e_4 & e_5 & e_6 & e_7 & e_8 & e_9 & e_{10} & e_{11} & e_{12} \end{bmatrix}^{\mathrm{T}} \tag{4}$$

The vector of nodal coordinates includes the global displacements

$$e_1 = r_1\big|_{x=0}, \qquad e_2 = r_2\big|_{x=0}, \qquad e_7 = r_1\big|_{x=l}, \qquad e_8 = r_2\big|_{x=l}$$

and the global slopes of the element nodes that are defined as

$$e_3 = \frac{\partial r_1}{\partial x}\bigg|_{x=0}, \qquad e_4 = \frac{\partial r_2}{\partial x}\bigg|_{x=0}, \qquad e_5 = \frac{\partial r_1}{\partial y}\bigg|_{x=0}, \qquad e_6 = \frac{\partial r_2}{\partial y}\bigg|_{x=0},$$

$$e_9 = \frac{\partial r_1}{\partial x}\bigg|_{x=l}, \qquad e_{10} = \frac{\partial r_2}{\partial x}\bigg|_{x=l}, \qquad e_{11} = \frac{\partial r_1}{\partial y}\bigg|_{x=l}, \qquad e_{12} = \frac{\partial r_2}{\partial y}\bigg|_{x=l}$$

The element shape function **S** must have a complete set of rigid body modes that describe arbitrary rigid body translational and rotational displacements. Using the element nodal coordinates given by Eq. 4, the element shape function can be defined as follows

$$\mathbf{S} = \begin{bmatrix} s_1 & 0 & ls_2 & 0 & ls_3 & 0 & s_4 & 0 & ls_5 & 0 & ls_6 & 0 \\ 0 & s_1 & 0 & ls_2 & 0 & ls_3 & 0 & s_4 & 0 & ls_5 & 0 & ls_6 \end{bmatrix} \tag{5}$$

where the functions $s_i = s(\xi, \eta)$ are defined as

$$s_1 = 1 - 3\xi^2 + 2\xi^3, \qquad s_2 = \xi - 2\eta^2 + \xi^3, \qquad s_3 = \eta - \xi\eta$$

$$s_4 = 3\xi^2 - 2\xi^3, \qquad s_5 = -\xi^2 + l\xi^3, \qquad s_6 = \xi\eta$$

and $\xi = \dfrac{x}{l}$, $\eta = \dfrac{y}{l}$, l is the element length.

3. CONSTANT MASS MATRIX

The global position vector of an arbitrary point on the shear-deformable beam is given by Eq. 3. By differentiating this equation with respect to time, the absolute velocity vector

can be defined as $\dot{\mathbf{r}} = \mathbf{S}\dot{\mathbf{e}}$. This vector can be used to define the kinetic energy of the element as

$$T = \frac{1}{2}\int_V \rho \dot{\mathbf{r}}^T \dot{\mathbf{r}} dV = \frac{1}{2}\dot{\mathbf{e}}^T \left(\int_V \rho \mathbf{S}^T \mathbf{S} dV \right) \dot{\mathbf{e}} = \frac{1}{2}\dot{\mathbf{e}}^T \mathbf{M}_a \dot{\mathbf{e}} \tag{6}$$

where V is the volume, ρ is the mass density of the beam material, and $\mathbf{M}_a$ is the mass matrix of the element. The mass matrix in Eq. 6 is constant and symmetric. Using the shape function given by Eq. 5, the mass matrix is given by

$$\mathbf{M}_a = \int_V \rho \mathbf{S}^T \mathbf{S} dV = \begin{bmatrix}
\frac{13}{35}m & 0 & \frac{11}{210}ml & 0 & \frac{7}{20}J_1 & 0 & \frac{9}{70}m & 0 & \frac{-13}{420}ml & 0 & \frac{3}{20}J_1 & 0 \\
0 & \frac{13}{35}m & 0 & \frac{11}{210}ml & 0 & \frac{7}{20}J_1 & 0 & \frac{9}{70}m & 0 & \frac{-13}{420}ml & 0 & \frac{3}{20}J_1 \\
\frac{11}{210}ml & 0 & \frac{1}{105}ml^2 & 0 & \frac{1}{20}J_1 l & 0 & \frac{13}{420}ml & 0 & \frac{-1}{140}ml^2 & 0 & \frac{1}{30}J_1 l & 0 \\
0 & \frac{11}{210}ml & 0 & \frac{1}{105}ml^2 & 0 & \frac{1}{20}J_1 l & 0 & \frac{13}{420}ml & 0 & \frac{-1}{140}ml^2 & 0 & \frac{1}{30}J_1 l \\
\frac{7}{20}J_1 & 0 & \frac{1}{20}J_1 l & 0 & \frac{1}{3}J_2 & 0 & \frac{3}{20}J_1 & 0 & \frac{-1}{30}J_1 l & 0 & \frac{1}{6}J_2 & 0 \\
0 & \frac{7}{20}J_1 & 0 & \frac{1}{20}J_1 l & 0 & \frac{1}{3}J_2 & 0 & \frac{3}{20}J_1 & 0 & \frac{-1}{30}J_1 l & 0 & \frac{1}{6}J_2 \\
\frac{9}{70}m & 0 & \frac{13}{420}ml & 0 & \frac{3}{20}J_1 & 0 & \frac{13}{35}m & 0 & \frac{-11}{210}ml & 0 & \frac{7}{20}J_1 & 0 \\
0 & \frac{9}{70}m & 0 & \frac{13}{420}ml & 0 & \frac{3}{20}J_1 & 0 & \frac{13}{35}m & 0 & \frac{-11}{210}ml & 0 & \frac{7}{20}J_1 \\
\frac{-13}{420}ml & 0 & \frac{-1}{140}ml^2 & 0 & \frac{-1}{30}J_1 l & 0 & \frac{-11}{210}ml & 0 & \frac{1}{105}ml^2 & 0 & \frac{-1}{20}J_1 l & 0 \\
0 & \frac{-13}{420}ml & 0 & \frac{-1}{140}ml^2 & 0 & \frac{-1}{30}J_1 l & 0 & \frac{-11}{210}ml & 0 & \frac{1}{105}ml^2 & 0 & \frac{-1}{20}J_1 l \\
\frac{3}{20}J_1 & 0 & \frac{1}{30}J_1 l & 0 & \frac{1}{6}J_2 & 0 & \frac{7}{20}J_1 & 0 & \frac{-1}{20}J_1 l & 0 & \frac{1}{3}J_2 & 0 \\
0 & \frac{3}{20}J_1 & 0 & \frac{1}{30}J_1 l & 0 & \frac{1}{6}J_2 & 0 & \frac{7}{20}J_1 & 0 & \frac{-1}{20}J_1 l & 0 & \frac{1}{3}J_2
\end{bmatrix} \tag{7}$$

where m is the total mass of the finite element, l is the element length, J_1 is the first moment of mass defined as $J_1 = \int_V \rho y dV$, and J_2 is the second moment of mass defined as $J_2 = \int_V \rho y^2 dV$.

4. ELASTIC FORCES

In this section, the nonlinear strain-displacement relations are used to develop an expression for the elastic forces of the beam element. The deformation gradient can be defined as [2]

$$\mathbf{J} = \frac{\partial \mathbf{r}}{\partial \mathbf{x}} = \begin{bmatrix} \dfrac{\partial r_1}{\partial x} & \dfrac{\partial r_1}{\partial y} \\ \dfrac{\partial r_2}{\partial x} & \dfrac{\partial r_2}{\partial y} \end{bmatrix} = \begin{bmatrix} \mathbf{S}_{1x}\mathbf{e} & \mathbf{S}_{1y}\mathbf{e} \\ \mathbf{S}_{2x}\mathbf{e} & \mathbf{S}_{2y}\mathbf{e} \end{bmatrix} \tag{8}$$

where $\mathbf{S}_{ix} = \dfrac{\partial \mathbf{S}_i}{\partial x}$, $\mathbf{S}_{iy} = \dfrac{\partial \mathbf{S}_i}{\partial y}$ and $\mathbf{S}_i$ is the i th row of the element shape function. The Lagrangian strain tensor ε_m can be written as

$$\varepsilon_m = \frac{1}{2}\left(\mathbf{J}^T\mathbf{J} - \mathbf{I}\right) = \frac{1}{2}\begin{bmatrix} \mathbf{e}^T\mathbf{S}_a\mathbf{e} - 1 & \mathbf{e}^T\mathbf{S}_c\mathbf{e} \\ \mathbf{e}^T\mathbf{S}_c\mathbf{e} & \mathbf{e}^T\mathbf{S}_b\mathbf{e} - 1 \end{bmatrix} \tag{9}$$

where $\mathbf{I}$ is the identity matrix, $\mathbf{S}_a = \mathbf{S}_{1x}^T\mathbf{S}_{1x} + \mathbf{S}_{2x}^T\mathbf{S}_{2x}$, $\mathbf{S}_b = \mathbf{S}_{1y}^T\mathbf{S}_{1y} + \mathbf{S}_{2y}^T\mathbf{S}_{2y}$, and $\mathbf{S}_c = \mathbf{S}_{1x}^T\mathbf{S}_{1y} + \mathbf{S}_{2x}^T\mathbf{S}_{2y}$. It should be noted that strain tensor is symmetric thus it can written in a vector form as

$$\varepsilon = \begin{bmatrix} \varepsilon_1 & \varepsilon_2 & \varepsilon_3 \end{bmatrix}^T \tag{10}$$

where $\varepsilon_1 = \frac{1}{2}(\mathbf{e}^T\mathbf{S}_a\mathbf{e} - 1)$, $\varepsilon_2 = \frac{1}{2}(\mathbf{e}^T\mathbf{S}_b\mathbf{e} - 1)$, and $\varepsilon_3 = \frac{1}{2}\mathbf{e}^T\mathbf{S}_c\mathbf{e}$.

A general expression for the strain energy can be written using the strain vector ε and the stress vector $\sigma = \begin{bmatrix} \sigma_1 & \sigma_2 & \sigma_3 \end{bmatrix}^T$ as follows [4, 5]

$$U = \frac{1}{2}\int_V \sigma^T \varepsilon \, dV \tag{11}$$

Using the constitutive equations, the stress vector is related to the strain vector by

$$\boldsymbol{\sigma} = \mathbf{E}\boldsymbol{\varepsilon} \tag{12}$$

where **E** is the matrix of the elastic constants of the material. For isotropic homogenous material, the matrix **E** can be expressed in terms of Lame's constants λ and μ as

$$\mathbf{E} = \begin{bmatrix} \lambda+2\mu & \lambda & 0 \\ \lambda & \lambda+2\mu & 0 \\ 0 & 0 & 2\mu \end{bmatrix} \tag{13}$$

where $\lambda = \dfrac{E\nu}{(1+\nu)(1-2\nu)}$, $\mu = \dfrac{E}{2(1+\nu)}$, E is the Young's modulus of elasticity, and ν is the Poisson's ratio of the beam material. Using Eqs. 12 and 13, the strain energy can be rewritten as

$$U = \frac{1}{2}\int_V \boldsymbol{\varepsilon}^T \mathbf{E}\boldsymbol{\varepsilon}\, dV \tag{14}$$

The vector of the elastic forces $\mathbf{Q}_e$ can be defined using the strain energy U as

$$\mathbf{Q}_e^T = \frac{\partial U}{\partial \mathbf{e}} = \mathbf{e}^T\mathbf{K} \tag{15}$$

where **K** is the stiffness matrix which can be written as

$$\mathbf{K} = (\lambda+2\mu)\mathbf{K}_1 + \lambda\,\mathbf{K}_2 + 2\mu\,\mathbf{K}_3 \tag{16}$$

where

$$\mathbf{K}_1 = \frac{1}{4}\int_V \left[\mathbf{S}_{a1}(\mathbf{e}^T\mathbf{S}_a\mathbf{e}-1) + \mathbf{S}_{b1}(\mathbf{e}^T\mathbf{S}_b\mathbf{e}-1)\right] dV,$$

$$\mathbf{K}_2 = \frac{1}{4}\int_V \left[\mathbf{S}_{a1}(\mathbf{e}^T\mathbf{S}_b\mathbf{e}-1) + \mathbf{S}_{b1}(\mathbf{e}^T\mathbf{S}_a\mathbf{e}-1)\right] dV,$$

$$\mathbf{K}_3 = \frac{1}{4}\int_V \mathbf{S}_{c1}(\mathbf{e}^T\mathbf{S}_a\mathbf{e})\, dV,$$

$$\mathbf{S}_{a1} = \mathbf{S}_a + \mathbf{S}_a^T,\ \mathbf{S}_{b1} = \mathbf{S}_b + \mathbf{S}_b^T,\ \text{and}\ \mathbf{S}_{c1} = \mathbf{S}_c + \mathbf{S}_c^T.$$

Note that the general expression for the elastic forces obtained in this investigation using the continuum mechanics approach and the nonlinear strain-displacement relationships is much simpler than the expression obtained in previous investigations [6, 9] using the element local coordinate system and linear strain-displacement relationships. The general expression obtained in this paper automatically captures the effect of geometric centrifugal stiffening.

5. FORMULATION OF THE GENERALIZED EXTERNAL FORCES

The virtual work can be used to develop the vector of the generalized external forces [10]. The virtual work due to an externally applied force $\mathbf{F}$ acting on an arbitrary point on the element is given by

$$\delta W_e = \mathbf{F}^T\delta\mathbf{r} = \mathbf{F}^T\,\mathbf{S}\,\delta\mathbf{e} = \mathbf{Q}_e^T\delta\mathbf{e} \tag{17}$$

where $\mathbf{r}$ is the position vector of the point of application of the force, and $\mathbf{Q}_e = \mathbf{S}^T\mathbf{F}$ is the vector of the generalized forces associated with the element nodal coordinates. For example, the virtual work due to the distributed gravity of the finite element can be obtained using the shape function and Eq. 17 as

$$\int_V [0 \quad -\rho g]\mathbf{S}\,\delta\mathbf{e} = -mg\begin{bmatrix}0 & \frac{1}{2} & 0 & \frac{l}{12} & 0 & 0 & 0 & \frac{1}{2} & 0 & -\frac{l}{12} & 0 & 0\end{bmatrix}\delta\mathbf{e} \tag{18}$$

This defines the vector of generalized distributed gravity forces as

$$\mathbf{Q}_e = -mg\begin{bmatrix}0 & \frac{1}{2} & 0 & \frac{l}{12} & 0 & 0 & 0 & \frac{1}{2} & 0 & -\frac{l}{12} & 0 & 0\end{bmatrix}^T \tag{19}$$

When an external moment M acts on the cross-section of the beam, the virtual work due to this moment is given by

$$\delta W_M = M\,\delta\gamma \tag{20}$$

where γ is the angle of rotation of the cross-section. The orientation of a coordinate system attached to the cross-section can be defined using the following transformation matrix

$$\begin{bmatrix} \cos(\gamma) & -\sin(\gamma) \\ \sin(\gamma) & \cos(\gamma) \end{bmatrix} = \frac{1}{f}\begin{bmatrix} \dfrac{\partial r_2}{\partial y} & \dfrac{\partial r_1}{\partial y} \\ \dfrac{-\partial r_1}{\partial y} & \dfrac{\partial r_2}{\partial y} \end{bmatrix}, \qquad f = \sqrt{\left(\frac{\partial r_1}{\partial y}\right)^2 + \left(\frac{\partial r_2}{\partial y}\right)^2} \tag{21}$$

which yields

$$\cos(\gamma) = \frac{1}{f}\frac{\partial r_2}{\partial y}, \qquad \sin(\gamma) = -\frac{1}{f}\frac{\partial r_1}{\partial y} \tag{22}$$

Using these two equations, it can be shown that the virtual change in the cross-section orientation angle can be defined as

$$\delta\gamma = \frac{\dfrac{\partial r_2}{\partial y}\,\delta\left(\dfrac{\partial r_1}{\partial y}\right) - \dfrac{\partial r_1}{\partial y}\,\delta\left(\dfrac{\partial r_2}{\partial y}\right)}{f^2} \tag{23}$$

If a concentrated moment is applied for example at node A as shown in Fig. 4, the generalized force vector due to this moment is defined as,

$$\mathbf{Q}_M = \begin{bmatrix} 0 & 0 & 0 & 0 & \dfrac{Me_6}{f_A^2} & \dfrac{-Me_5}{f_A^2} & 0 & 0 & 0 & 0 & 0 & 0 \end{bmatrix}^T \tag{24}$$

6. NUMERICAL EXAMPLES

Using the obtained expressions of the elastic and inertia forces, the equations of motion can be obtained using the absolute nodal coordinates as

$$\mathbf{M}_a\ddot{\mathbf{e}} = \mathbf{Q} \tag{25}$$

where $\mathbf{Q}$ is the vector of generalized nodal forces including the elastic force vector $\mathbf{Q}_e$ and external force vector $\mathbf{Q}_k$, and $\ddot{\mathbf{e}}$ is the vector absolute accelerations. As previously mentioned, the centrifugal and Coriolis force vectors are equal to zero since the mass matrix is constant.

In this section, two examples are considered in order to demonstrate the performance of the proposed beam model. The two examples considered are the free falling of a flexible pendulum under its own weight, and a four bar mechanism with a flexible connecting rod.

The first example considered is the free falling two-dimensional beam shown in Fig. 5. The beam is connected to the ground by a pin joint at one end. The beam has length of 1.2 m, circular cross-sectional area of 0.0016 m^2, second moment area 8.533E-06, a mass density of 5540 kg/m^3, Poisson's ratio of 0.3, and a modulus of elasticity of 0.700E 06. The beam is initially horizontal with zero initial velocity and free to fall under the effect of gravity. Two cases are considered in this example. In the first case, the gravity constant is assumed to be 9.81 m/s^2 while in the second case, the gravitational acceleration is increased to 50 m/s^2. The simulations of the beam are performed using different number of elements. Figure 6 shows the position of the tip point of the beam using 6 and 12 finite elements when the gravity constant is equal to 9.81 m/s^2. It is clear from the results presented in this figure that there is a good agreement between the two models. The results demonstrate that the solution converges with small number of elements.

Since the falling pendulum is conservative system, the sum of the energy components must remains constant, that is

$$\sum_{i}^{ne} T^i + U^i + V^i = const \tag{26}$$

where T^i is the element kinetic energy, U^i is the element strain energy, V^i is the element potential energy, and *ne* is the number of elements of the system. Figure 7 shows the energy balance for 6-element model. The results presented in this figure shows that the total energy remains constant. The results obtained using the 6-element model are the same as the results of the 12-element model. Figure 8 shows the displacement of the tip point of both models under gravitational acceleration of 50 m/s^2. Very small differences between the two models can be observed. The energy balance obtained using the 6-element model under the gravity constant of 50 m/s^2 is shown in Fig 9. The same results are obtained using the 12-element model. Figure 10 shows the large deformation configurations of the falling beam at different time steps under gravitational acceleration of 50 m/s^2 using 48 finite elements.

The shear-deformable model developed in this investigation relaxes the assumption of Euler-Bernoulli beam theory. In this model, the cross-section does not remain perpendicular to the beam centerline due to the effect of the shear deformation. Figure 11 shows a comparison between the results obtained using this new model and the Euler-Bernoulli beam model previously presented by Berzeri et al [3] who used a shape function which does not depend on y. The results obtained in this figure are obtained using 12 elements. It is important to point out that the shear-deformable model, because of the dependence of the shape function on y, leads to a simpler expression for the elastic forces. More surprisingly, significant saving in computer time was achieved using the shear-deformable model. It was observed that the shear-deformable model is two times faster than the Euler-Bernoulli model. The results presented in Fig. 11 shows that there is a very good agreement between the shear-deformable beam model and the model based on the Euler-Bernoulli beam theory since a thin beam is used. When the cross-section changed to 0.001 m^2 and second moment area 1.593E-06 m^4, noticeable differences are observed as shown in Fig. 12.

The shear-deformable model developed in this investigation also relaxes the assumption of the Timoshenko beam theory since it allows for the plane deformation of

the cross-section, that is the cross-section remains plane but not rigid. The deformation of the cross-section can be measured by the deviation of the norm of the vector $\partial \mathbf{r} / \partial y$ from one. Figure 13 shows the norm of this vector at node 5 and node 9 as a function of time in the case of free falling pendulum and gravity constant of 50 m/s^2.

The second example considered in this numerical study is the four bar mechanism. The mechanism consists of a rigid crankshaft, a flexible connecting rod, and a flexible follower. The initial configuration of the mechanism is shown in Fig. 14. The geometric and inertia properties of the four bar mechanism are shown in Table 1. The crankshaft is driven by a moment defined by the function shown in Fig. 15. In this simulation, one element is used for the crankshaft, 6 elements for the connecting rod, and 4 elements for the follower. The longitudinal and transverse deflection of the mid point of the connecting rod is shown in Fig. 16. Also, for this multibody example the solution converges with small number of elements.

7. SUMMARY AND CONCLUSIONS

In this investigation, a shear-deformable beam model based on the non-incremental absolute nodal coordinate formulation is developed for the large rotation and large deformation analysis. The beam model leads to exact modeling of the rigid body dynamics and leads to zero strain under an arbitrary rigid body displacement. Furthermore, the model relaxes the assumptions of Euler-Bernoulli and Timoshenko beam theories. The cross-section in the new model does not remain rigid and does not remain perpendicular to the beam centerline. By using a continuum mechanics approach, the model leads to a relatively simple expression for the elastic force.

While the model accounts for the effect of the rotary inertia and shear deformation, the mass matrix remains constant. As a consequence, the centrifugal and Coriolis forces are identically equal to zero. Two numerical examples, a free falling pendulum and a multibody four bar mechanism, were used to demonstrate the use of the new beam model. Numerical results obtained in this study demonstrated that the solutions obtained using the new model converges much faster as compared to the non-shear-deformable models presented in previous investigations. Furthermore, significant saving

in computer time is achieved by using the more general shear-deformable model that is based on the nonlinear strain-displacement relationships.

ACKNOWLEDGMENT

This research was supported by the U.S. Army Research Office, Research Triangle Park, NC.

REFERENCES

1. Bath, K. J., 1996, Finite Element Procedures, Prentice Hall, Englewood Cliffs, New Jersey.
2. Bonet, J., Wood, R. D., 1997, Nonlinear Continuum Mechanics for Finite Element Analysis, Cambridge University Press, Cambridge.
3. Berzeri, M., Shabana, A., A., 1999, " A Continuum Mechanics Approach for Formulating the Elastic Forces in the Absolute Nodal Coordinate Formulation," Technical Report MBS99-3-UIC, University of Illinois at Chicago, IL.
4. Crisfield, M. A., 1997, Nonlinear Finite Element Analysis of Solids and Structures, John Wiley & Sons, England.
5. Dym, C. L., and Shames, I. H., 1973, Solid Mechanics, A Variational Approach, McGraw-Hill, Inc.
6. Escalona, J. L., Hussien, A. H. and Shabana, A., A., 1998, " Application of the Absolute Nodal Coordinates Formulation to Multibody System Dynamics," Journal of Sound and Vibration, 214, No. 5, pp. 833-851.
7. Greenberg, M.D., 1998, Advanced Engineering Mathematics, 2nd edition, Prentice Hall, Upper Saddle River, New Jersey.
8. Shabana, A., A., 1996, "An Absolute Nodal Coordinates Formulation for the Large Rotation and Deformation Analysis of Flexible Bodies," Technical Report MBS96-1-UIC, University of Illinois at Chicago, IL.

9. Shabana, A., A., 1998, " Computer Implementation of the Absolute Nodal Coordinates Formulation for Flexible Multibody Dynamics," Nonlinear Dynamics, 16, pp.293-306.

10. Shabana, A., A., 1998, Dynamics of Multibody Systems, 2nd edition, Cambridge University Press, Cambridge.

11. Shabana, A., A., Hussien, A. H. and Escalona, J. L., 1998, " Application of the Absolute Nodal Coordinates Formulation to Large Rotation and Large Deformation Problems," ASME Journal of Mechanical Design, 120, pp. 188-195.

12. Timoshenko, S. P., and Goodier, J. N., 1970, Theory of Elasticity, 3rd edition, McGraw-Hill, Inc.

13. Ugural, A. C., and Fenster, S. K., 1995, Advanced Strength and Applied Elasticity, 3rd edition, Prentice Hall, Upper Saddle River, New Jersey.

Table 1. The geometric and inertia properties of the four bar mechanism

Body	m (kg)	A (m^2)	I (m^4)	l (m)	E (Pa)	ν
Crankshaft	0.681	1.257E-03	1.257 E-07	0.200	1.000 E+09	0.3
Coupler	2.474	1.960 E-03	3.068 E-07	0.900	5.000 E+06	0.3
Follower	1.470	7.068 E-0	3.976 E-08	0.519	5.000 E+08	0.3

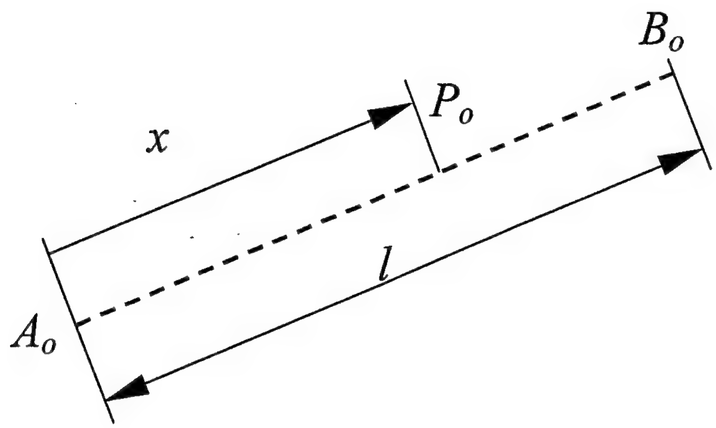

a) The beam in the undeformed configuration

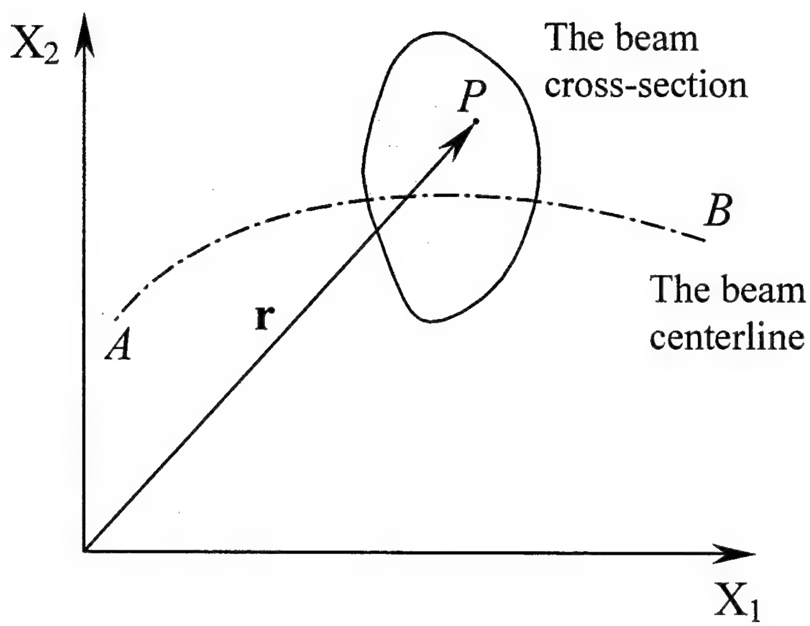

b) The beam in the deformed configuration

Fig. 1. The position vector of an arbitrary point on the beam cross-section

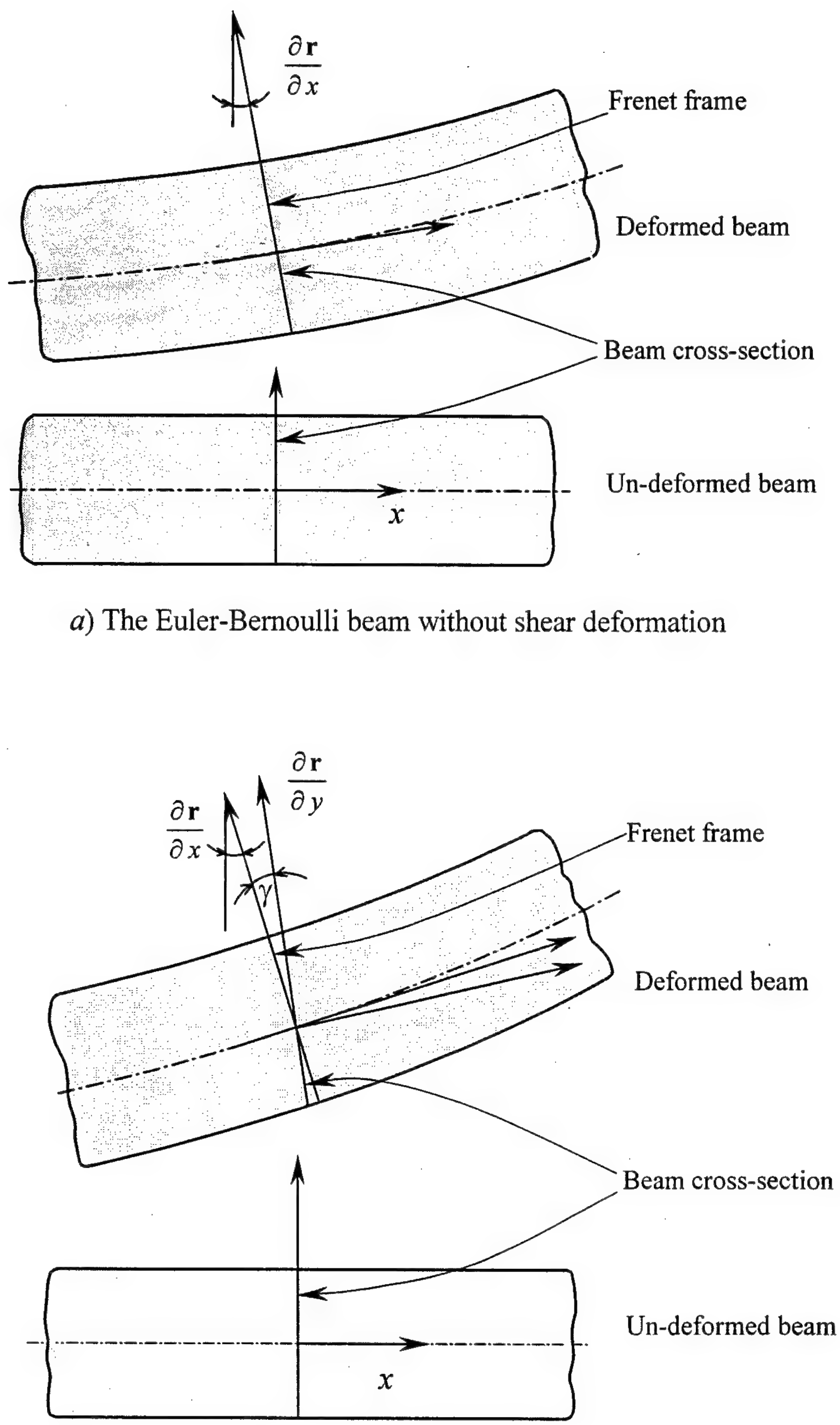

a) The Euler-Bernoulli beam without shear deformation

b) The beam element with shear deformation

Fig. 2. The beam deformation assumptions

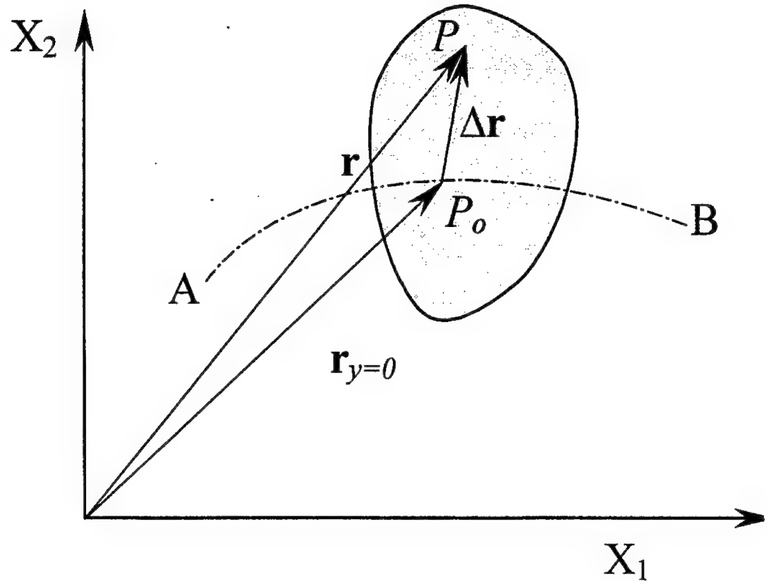

Fig. 3. The position vector of an arbitrary point on the beam cross-section

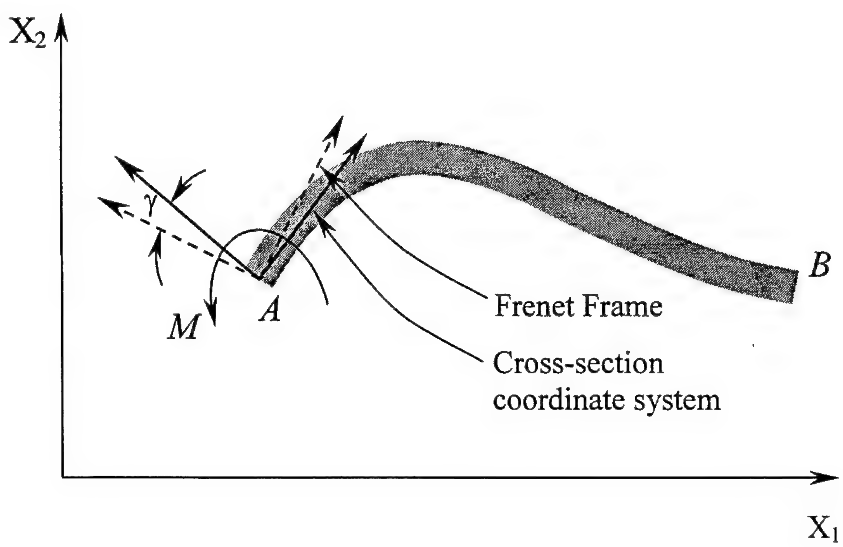

Fig. 4. Externally applied moment

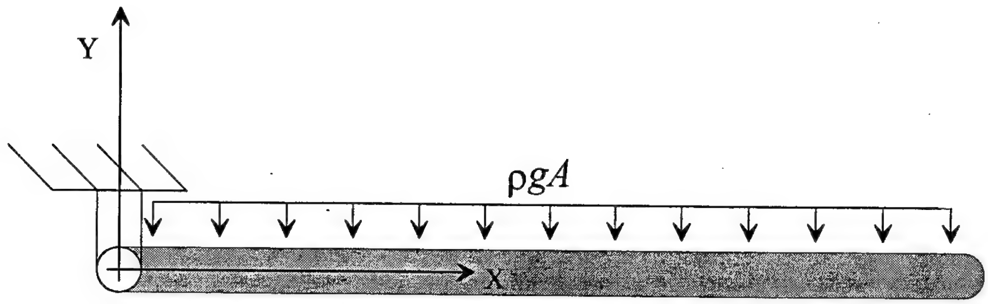

Fig. 5. Free falling flexible pendulum

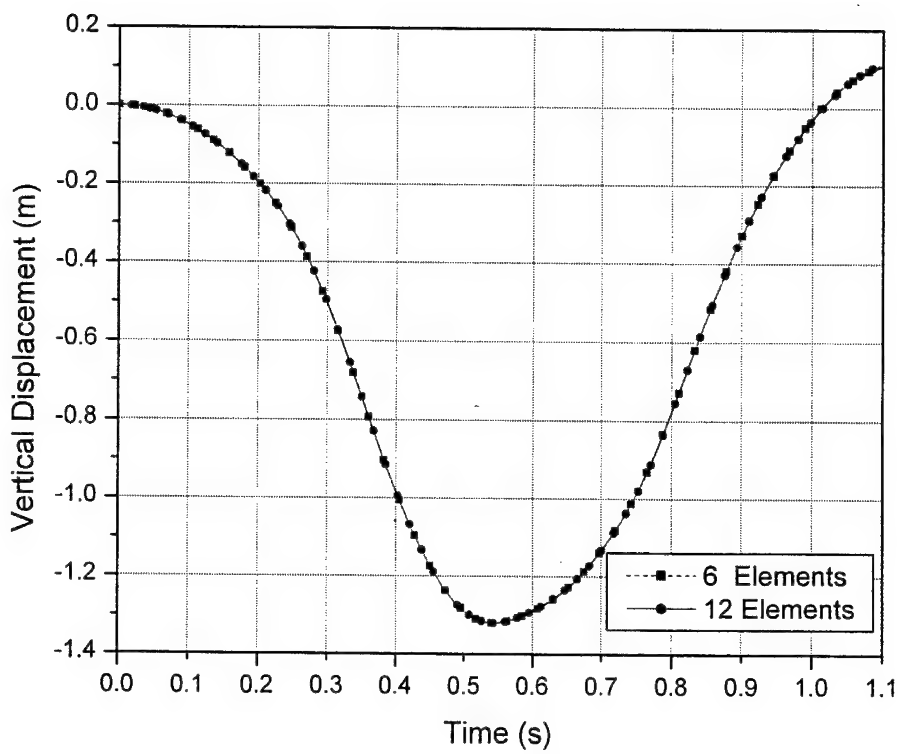

Fig. 6. Displacement of the beam tip point using 6 and 12 elements beam under acceleration 9.81 m/s^2

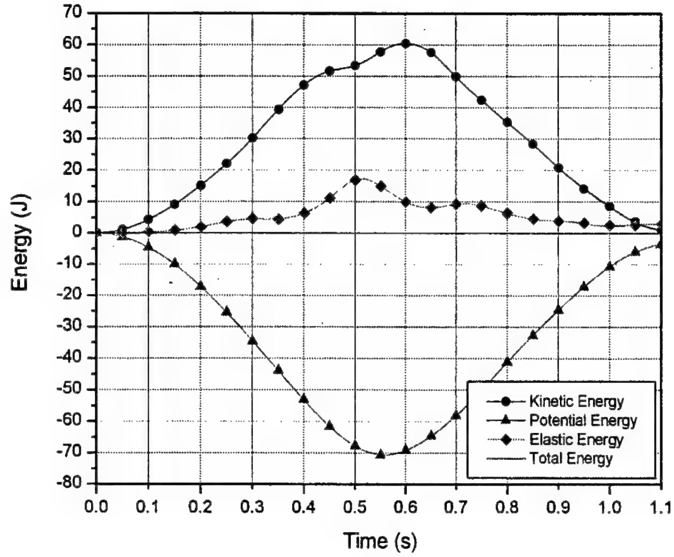

Fig. 7. Energy balance of the beam ($g = 9.81$ m/s^2)

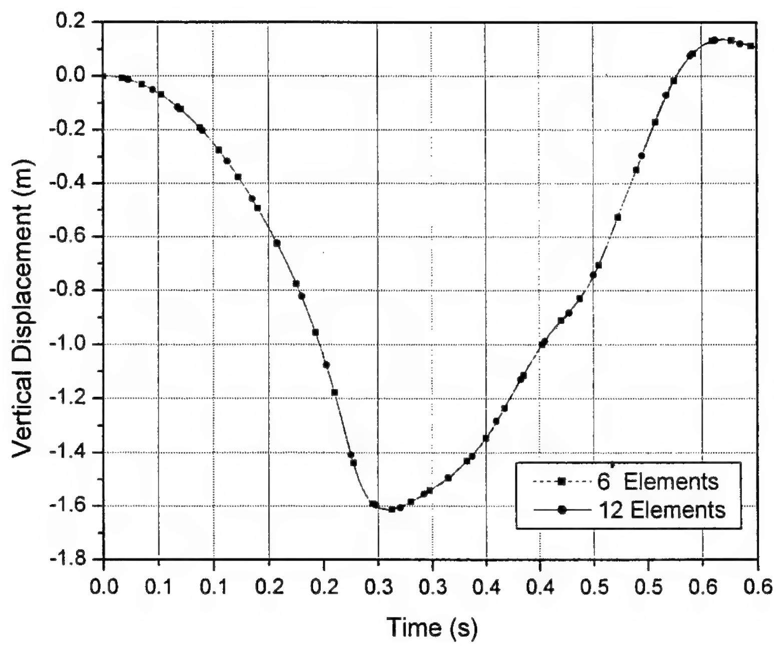

Fig. 8. Displacement of the beam tip point ($g = 50$ m/s^2)

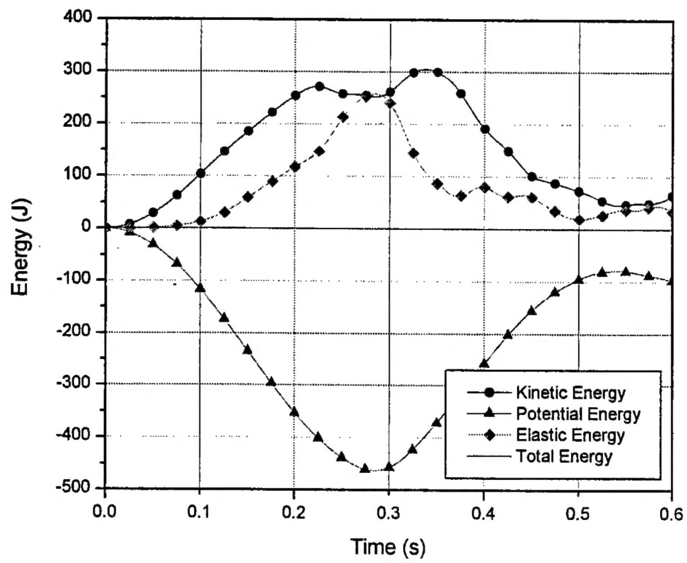

Fig. 9. Energy balance of the beam ($g = 50$ m/s^2)

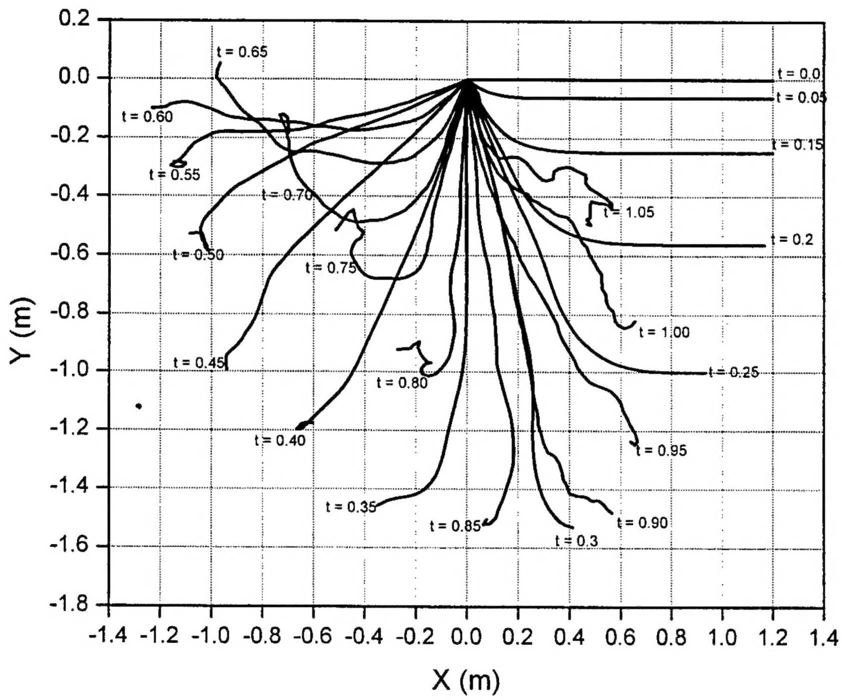

Fig. 10. The falling flexible pendulum at different time steps using 48 elements ($g = 50$ m/s^2)

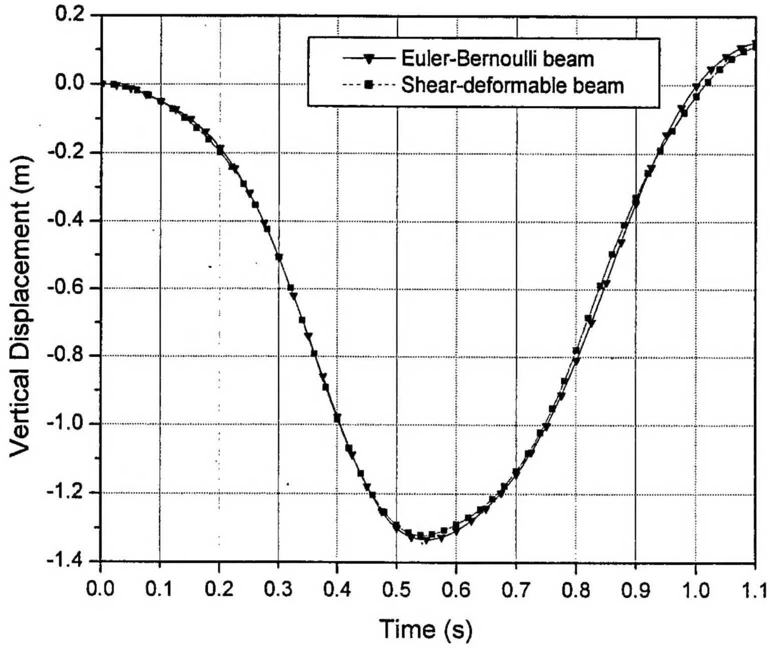

Fig. 11. Comparison between the results Euler-Bernoulli beam model and shear-deformable beam

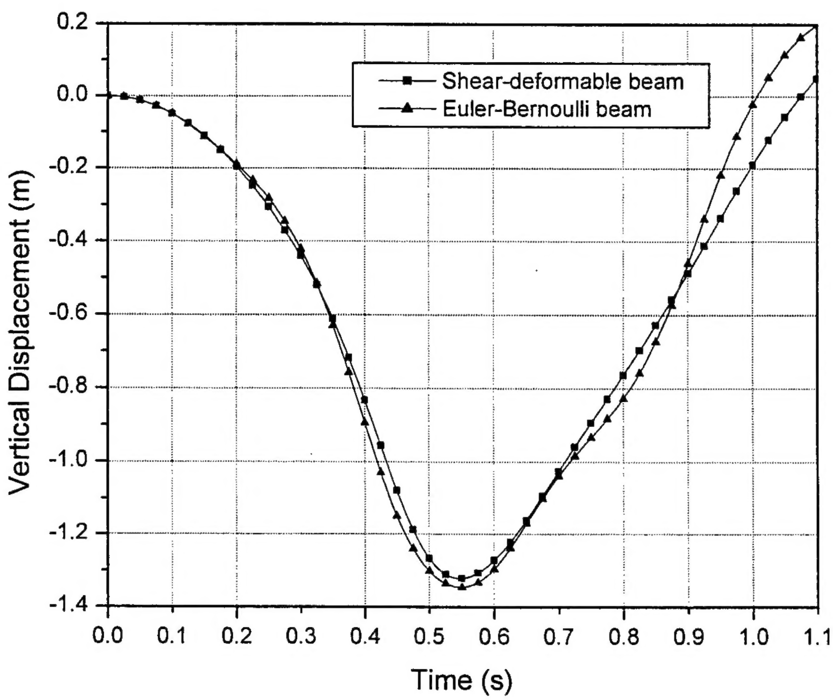

Fig. 12. Comparison between the results Euler-Bernoulli beam model and shear-deformable beam for thick cross-section

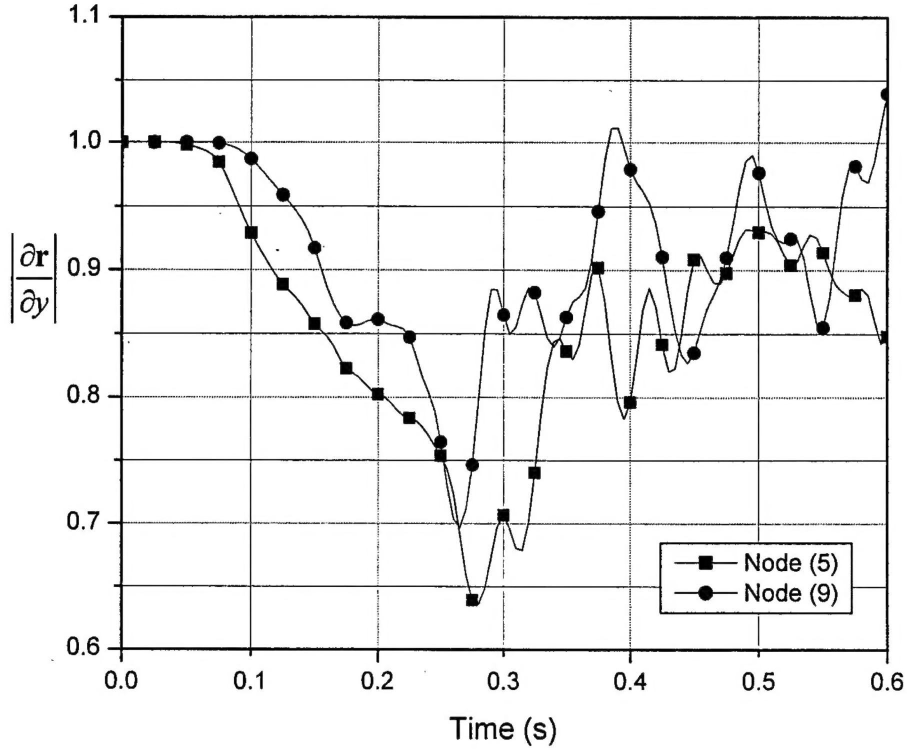

Fig. 13. The norm of the vector $\frac{\partial \mathbf{r}}{\partial y}$ as function of time

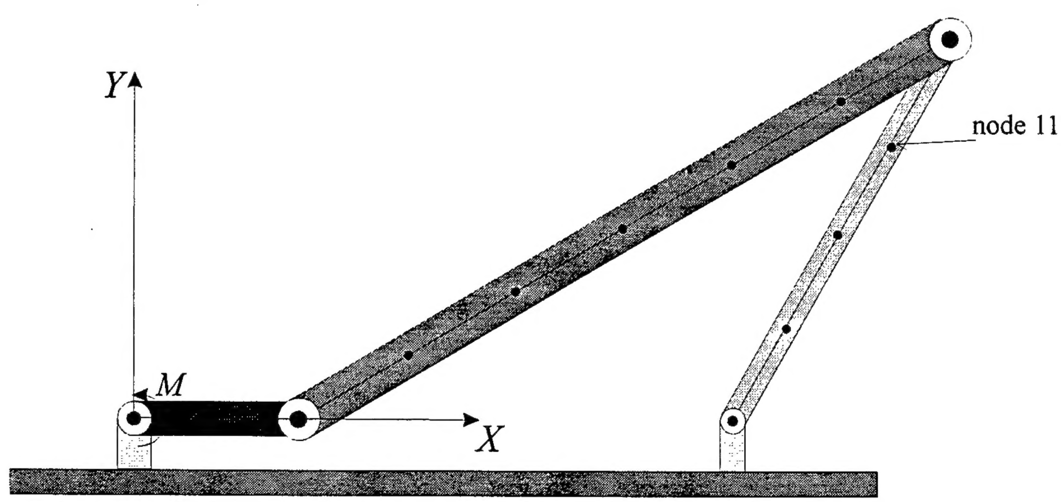

Fig. 14. The four-bar mechanism at the initial configuration

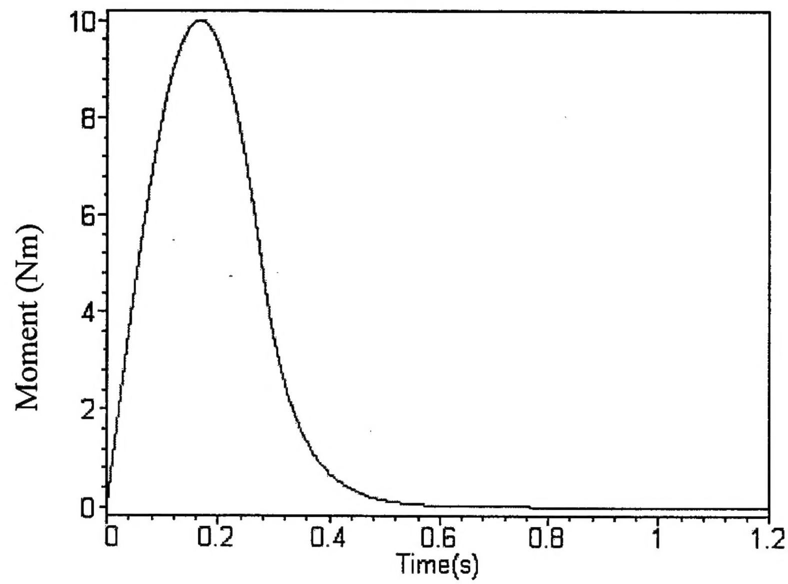

Fig. 15. The driving moment applied to the crankshaft

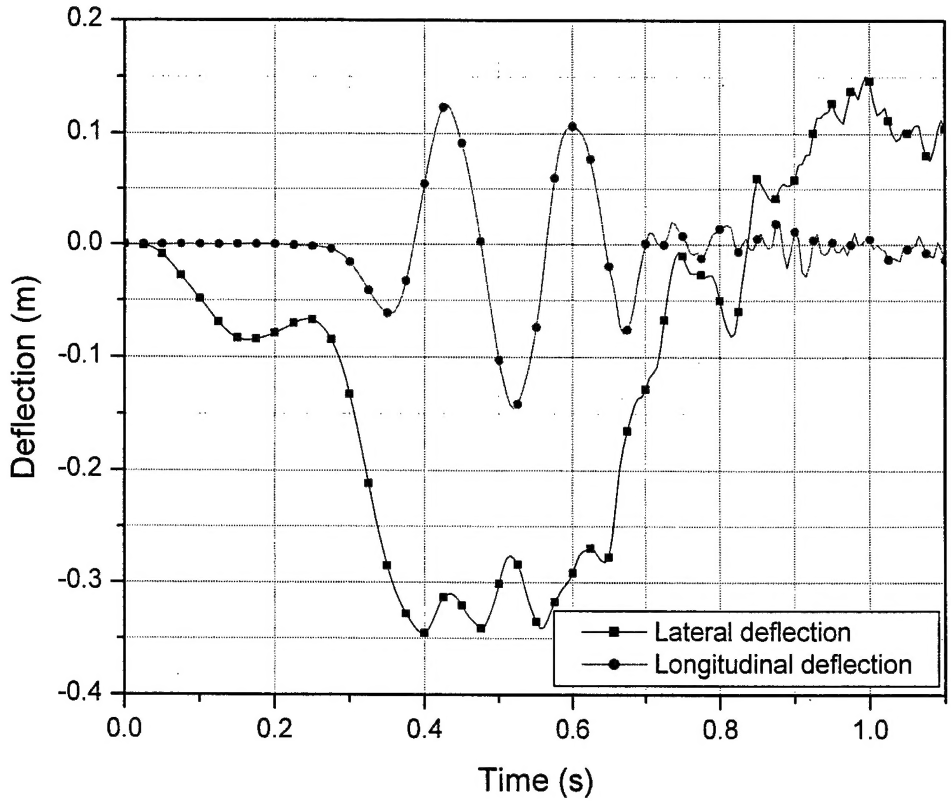

Fig. 16. The longitudinal and lateral deformation of the mid point of the coupler link